Location-based User Scheduling through Graph Coloring for Cell-Free MIMO NTN Systems

Location-based User Scheduling through Graph Coloring for Cell-Free MIMO NTN Systems

Daniel Gaetano Riviello*, Bruno De Filippo*, Bilal Ahmad*, Alessandro Guidotti†, Alessandro Vanelli-Coralli*
*Dept. of Electrical, Electronic, and Information Engineering (DEI), Univ. of Bologna, Bologna, Italy
†National Inter-University Consortium for Telecommunications (CNIT), Bologna, Italy
{daniel.riviello, bruno.defilippo, bilal.ahmad6, a.guidotti, alessandro.vanelli}@unibo.it

***Abstract*—Non-Terrestrial Networks (NTN) have recently grown in popularity, with Low Earth Orbit (LEO) mega-constellations delivering broadband services to households worldwide. Under the cell-free MIMO paradigm in full frequency reuse systems, meeting the increasing traffic demand requires complex scheduling and digital beamforming algorithms to minimize the excessive co-channel interference. In this paper, we present a user scheduling algorithm for LEO-based B5G NTNs with reduced computational complexity that does not require knowledge of downlink (DL) Channel State Information (CSI). In our proposed method, we perform user grouping by first solving the Minimum Clique Cover (MCC) problem on an inter-user distance adjacency matrix, avoiding the need for DL pilots for CSI estimation. We approach MCC as a graph coloring task on the complementary graph, using the DSatur algorithm to minimize the computational complexity of the scheduler. Users within the same group are served via space-division multiplexing by means of feed space digital beamforming, inferring the users' channel vectors from their position. System-level analysis show that the proposed algorithm, named Distance-based MCC DSatur (D-MCC-DSatur), achieves a per-cluster sum-rate capacity gain of up to 1.8% with respect to the distance-based Multiple Antenna Downlink User Scheduling (D-MADOC) algorithm.**

***Index Terms*—User Scheduling, Non-Terrestrial Networks, Cell-Free MIMO, Graph Coloring, Beamforming**

I. Introduction

During the most recent years, Satellite Communications (SatCom) have become one of the most discussed topics for the wireless networks of the future. Under the denomination of "Non-Terrestrial Networks", the Third Generation Partnership Project (3GPP) has included SatCom into its standardization activities, with the first set of NTN-specific Technical Specification published in Release 17 [1]. Driven by the promise of a global coverage with minimal latency, Low Earth Orbit (LEO) NTN have grown in popularity over traditional Geostationary Earth Orbit (GEO) SatCom systems. Few LEO mega-constellations have already reached the operational status, *e.g.*, Eutelsat's OneWeb and SpaceX's Starlink, with further systems being planned for launch within the current decade, *e.g.*, Amazon's Kuiper and the European Union's IRIS^2. Nonetheless, the high mobility that characterizes satellites in LEO poses several challenges, among which is the management of the available spectrum for SatCom. In order to enhance the spectral efficiency, Full Frequency Reuse (FFR) can be implemented [2], resulting in the same frequency band being allocated to each NTN cell. Among the paradigms currently being investigated, Cell-Free (CF) communication systems have also been identified as a potential source of spectral efficiency improvement, freeing the SatCom system from the requirement of a definition of an on-ground beam lattice. The co-channel interference typically introduced with these paradigms can be mitigated through Feed Space (FS) digital beamforming. Here, a subset of users can be scheduled within each time slot and served in downlink (DL) using Space Division Multiplexing (SDM), maximizing the resource usage [3]. However, the beamformers' performance has a strong dependence on the user spatial arrangement and Channel State Information (CSI), leading to the need to investigate user scheduling techniques. In the current State-of-the-Art, suboptimal solutions can be found aiming at balancing complexity and performance, *e.g.*, [4]–[6]. In [4], the authors designed user scheduling algorithms from the geometric point of view to take into account the different SNR and number of antennas at each User Terminal (UT). The authors in [5] proposed the Sum-rate Maximization User Grouping (SMUG) algorithm, which chooses the set of UTs to serve within the same time slot by iteratively adding to the group the UT that would lead to the largest sum-rate increase. Finally, [6] presents the Multiple Antenna Downlink Orthogonal Clustering (MADOC) algorithm, in which a channel correlation metric is used as a group policy, creating group of users which pairwise correlation does not exceed an optimized threshold.

In this paper, we extend our previous works [7]–[9] by presenting a user scheduling approach in a CF-MIMO LEO-based NTN by means of an undirected, unweighted graph, based on the users' position and not on DL CSI. The proposed method approaches the Minimum Clique Cover (MCC) problem as a graph coloring task on the complementary graph, aiming at reducing the Radio Resource Management (RRM) algorithms' complexity. Once user clusters are formed, the largest ones are selected for transmission during the upcoming scheduling frame, where users are served by means of SDM using FS Location-Based Minimum Mean Squared Error (LB-MMSE) beamforming. To optimize system performance, we perform a heuristic search for the threshold value that maximizes the per-cluster sum-rate capacity for several power normalization techniques, *i.e.*, Sum-Power-Constraint (SPC), Maximum-Power-Constraint (MPC), and a variation of the Per-Antenna-Constraint (PAC). We report in Tab. I the terminology and notation used throughout the paper, along with their description.

TABLE I
ADOPTED TERMINOLOGY AND NOTATION

$\mathbf{A}^\intercal$	Transpose of matrix $\mathbf{A}$
$\mathbf{A}^H$	Conjugate transpose of matrix $\mathbf{A}$
$\text{diag}(\mathbf{A})$	Vector containing diagonal elements of $\mathbf{A}$
$\text{diag}(\mathbf{a})$	Diagonal matrix constructed from vector $\mathbf{a}$
$[\mathbf{A}]_{i,j}$	Element at row i and column j of matrix $\mathbf{A}$
N_H, N_V	No. of array elements in y and z axis
$N_F = N_H \cdot N_V$	Total no. of array elements
d_H, d_V	Inter-element distance on y and z axis
κ	Boltzmann constant
B	User bandwidth
$T_i = T$	Equivalent noise temperature of UT i
d_i	Slant range of UT i
λ	Carrier wavelength
$k_0 = 2\pi\lambda$	Wave number
$g_E(\vartheta, \varphi)$	Radiation pattern of antenna elements
$G_i^{(rx)}$	Reception antenna gain for UT i
$\mathbf{I}_K$	$K \times K$ identity matrix
P_{tot}	Total onboard transmitting power
L_i	Additional propagation losses for UT i
T_{max}	No. of time slots per scheduling frame
$\alpha = \frac{N}{P_{tot}}$	Regularisation factor

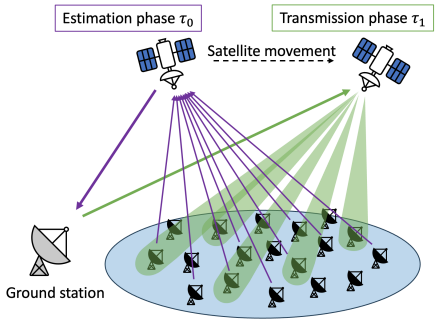

Fig. 1. LEO NTN system architecture.

II. System Model

The system model is adopted from our prior works [7]–[9] for consistency; readers can refer to [9] for a more detailed description. We consider a standalone LEO satellite with digital beamforming capabilities, equipped with an antenna array consisting of N_F radiating elements, serving K uniformly distributed on-ground UTs. The serving gNB, which is assumed to be located on ground and in the satellite's visibility, has the task of scheduling multiple transmissions in each scheduling frame, serving users through SDM using FS digital beamforming techniques at the satellite side. In order to perform such tasks, the gNB typically transmits pilots at time τ_0 to let users estimate their DL CSI, which are in turn forwarded to the gNB to determine the optimal user schedule. However, this operation introduces overhead in the communication, which reduces the overall throughput that the system can achieve. Hence, as shown in Fig. 1, we assume that, at each scheduling window, the GNSS-equipped UT i communicates to the gNB its estimated position at time τ_0 instead of DL CSI, eliminating the need for scheduling-dedicated DL pilots.

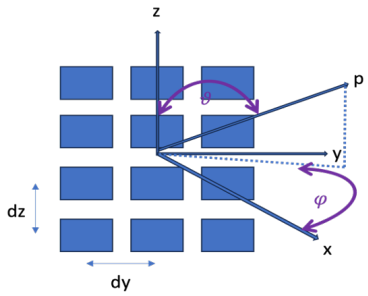

Fig. 2. Planar antenna array model.

Such data is then processed by RRM functions, resulting in the transmission of the scheduled symbols from the satellite at time $\tau_1 = \tau_0 + \Delta\tau$. Clearly, the latency $\Delta\tau$ between the position estimation and the DL transmission hinders system performance, as the channel aging due to the satellite (and, possibly, user) movement may cause the computed scheduling and beamforming matrices to be suboptimal for the actual transmission channel. Such latency includes the maximum propagation delay on the UL user link in the coverage area ($\tau_{\text{UT,max}}$), the DL and UL propagation delays on the feeder link (both assumed to be equivalent to τ_{feeder}), processing delays incurring due to RRM (τ_p) and further additional system delays (τ_{ad}):

$$\Delta\tau = \tau_{\text{UT,max}} + 2\tau_{\text{feeder}} + \tau_p + \tau_{ad} \tag{1}$$

More specifically, we assume that the LEO satellite is equipped with a Uniform Planar Array (UPA) to serve UTs on ground. Conventionally, the antenna boresight coincides with the sub-satellite point, while any position that deviates from it can be identified by the pair of angles (ϑ, φ) as shown in Fig. 2. The array response of the UPA in the direction of the i-th UT (ϑ_i, φ_i) can be represented as the Kronecker product of the array responses of two Uniform Linear Arrays (ULAs) aligned on the y-axis and the z-axis, respectively. We first define the $1 \times N_H$ steering vector (SV) of the ULA along the y axis as $\mathbf{a}_H(\theta_i, \varphi_i)$ and the $1 \times N_V$ SV of the ULA along the z axis as $\mathbf{a}_V(\theta_i)$:

$$\mathbf{a}_H(\vartheta_i,\varphi_i) = \left[1, e^{jk_0 d_H \sin\vartheta_i \sin\varphi_i}, \ldots, e^{jk_0 d_H (N_H-1)\sin\vartheta_i \sin\varphi_i}\right] \tag{2}$$

$$\mathbf{a}_V(\vartheta_i) = \left[1, e^{jk_0 d_V \cos\vartheta_i}, \ldots, e^{jk_0 d_V (N_V-1)\cos\vartheta_i}\right] \tag{3}$$

In this context, [10] provides additional information about the configuration and array response. Under the assumption that the array is equipped with directional antenna elements, each characterized by the radiation pattern $g_E(\vartheta_i, \varphi_i)$, the $1 \times N_F$ SV of the UPA in the direction of the i-th UT can be expressed as:

$$\mathbf{a}(\vartheta_i, \varphi_i) = g_E(\vartheta_i, \varphi_i)(\mathbf{a}_H(\vartheta_i, \varphi_i) \otimes \mathbf{a}_V(\vartheta_i)) \tag{4}$$

As CSI is assumed not to be available at the gNB, the FS channel vector between the N_F radiating elements of the UPA

and the i-th UT can be inferred from the UT position by computing the slant range d_i and the UT direction (ϑ_i, φ_i):

$$\hat{\mathbf{h}}_i = G_i^{(rx)} \frac{\lambda}{4\pi d_i} \sqrt{\frac{1}{\kappa BT}} e^{-j\frac{2\pi}{\lambda}d_i} \mathbf{a}(\vartheta_i, \varphi_i) \tag{5}$$

where $G_i^{(rx)}$ is the maximum reception gain of the i-th UT's antenna, which is assumed to be a VSAT based on the 3GPP model reported in [12], pointed towards the satellite. Clearly, $\hat{\mathbf{h}}_i$ is based on deterministic components and does not take into account the statistical additional losses L_i experienced by the i-th UT, e.g., shadowing, scintillation, and atmospheric attenuation. Hence, the real FS channel vector can be written as:

$$\mathbf{h}_i = G_i^{(rx)} \frac{\lambda}{4\pi d_i} \sqrt{\frac{L_i}{\kappa BT}} e^{-j\frac{2\pi}{\lambda}d_i} \mathbf{a}(\vartheta_i, \varphi_i) \tag{6}$$

By collecting all K channel vectors, the $K \times N_F$ complex system-level channel matrix $\hat{\mathbf{H}}$ is constructed as $\hat{\mathbf{H}} = \left[\hat{\mathbf{h}}_1^\intercal, \hat{\mathbf{h}}_2^\intercal, \ldots, \hat{\mathbf{h}}_K^\intercal\right]^\intercal$. In this matrix, the k-th row represents the channel vector of the k-th user, while the n-th column contains the channel coefficients from the n-th feed to the K UTs.

Under the assumption of infinite traffic demand (*i.e.*, new UTs request traffic at each scheduling window, replacing those that have been served during the previous window), we limit the scheduling window to a frame of $T_{\max}$ time slots. To maximize the system performance within the scheduling frame, the RRM algorithm defines a possible partition $\{\mathcal{C}_1, \mathcal{C}_2, \ldots, \mathcal{C}_{T_{\max}}\}$ of the subset $\mathcal{U}_s \subseteq \mathcal{U}$, where $\mathcal{U}$ represents the set of UTs. $\mathcal{C}_t \subseteq \mathcal{U}_s$ is defined as "cluster", and $K_t = |\mathcal{C}_t|$ represents its cardinality, with $t = 1, \ldots, T_{\max}$. In the t-th time slot of the scheduling frame, users belonging to cluster $\mathcal{C}_t$ are selected, leading to the formation of a $K_t \times N_F$ complex scheduled channel matrix $\hat{\mathbf{H}}_t \subseteq \hat{\mathbf{H}}$, which contains only the rows of the scheduled users in the t-th cluster. The selected beamforming algorithm computes for each cluster a $N_F \times K_t$ complex beamforming matrix $\mathbf{W}_t = [\mathbf{w}_1^{(t)}, \mathbf{w}_2^{(t)}, \ldots, \mathbf{w}_{K_t}^{(t)}]$, where $\mathbf{w}_i^{(t)}$ denotes the $N_F \times 1$ beamformer designed for the i-th user in the t-th cluster. Matrix $\mathbf{W}_t$ projects the K_t-dimensional column vector $\mathbf{s}_t = [s_1, s_2, \ldots, s_{K_t}]^\intercal$, containing the unit-variance user symbols, onto the N_F-dimensional space defined by the antenna feeds. Thus, in the feed space, the computation of the beamforming matrix allows for the generation of a dedicated beam towards each user direction. The signal received by the i-th user of cluster t can be expressed as [9]:

$$y_i^{(t)} = \mathbf{h}_i \mathbf{w}_i^{(t)} s_i + \sum_{\substack{k=1 \\ k \neq i}}^{K_t} \mathbf{h}_i \mathbf{w}_k^{(t)} s_k + z_i^{(t)} \tag{7}$$

During the estimation phase, the user position at time τ_0 is used to calculate the channel matrix $\hat{\mathbf{H}}$, and obtain the scheduling and beamforming matrices $\mathbf{W}_t$. The beamformed symbols are then transmitted to users at time $\tau_0 + \Delta\tau$.

The Signal-to-Interference-plus-Noise ratio (SINR) for user i belonging to cluster t can be computed as:

$$\text{SINR}_i^{(t)} = \frac{\left\|\mathbf{h}_i \mathbf{w}_i^{(t)}\right\|^2}{1 + \sum\limits_{\substack{k=1 \\ k \neq i}}^{K_t} \left\|\mathbf{h}_i \mathbf{w}_k^{(t)}\right\|^2} \tag{8}$$

The per-cluster sum-rate capacity can then be assessed as:

$$S_t = B \sum_{i=1}^{K_t} \log_2\left(1 + \text{SINR}_i^{(t)}\right) \tag{9}$$

The beamforming matrix $\mathbf{W}_t$, computed on a cluster basis, is determined using the linear LB-MMSE equation:

$$\mathbf{W}_t = \hat{\mathbf{H}}_t^H (\hat{\mathbf{H}}_t \hat{\mathbf{H}}_t^H + \alpha \mathbf{I}_{K_t})^{-1} \tag{10}$$

It must be noted that the power emitted by the satellite and antenna in beamforming is a particularly challenging step and needs careful consideration [6]. For this work, we considered SPC, MPC and a modified version of PAC [3] to obtain each normalized beamforming matrix $\tilde{\mathbf{W}}_t$:

$$\tilde{\mathbf{W}}_t^{(SPC)} = \frac{\sqrt{P_{tot}}\mathbf{W}_t}{\sqrt{\text{tr}(\mathbf{W}_t \mathbf{W}_t^H)}} \tag{11}$$

$$\tilde{\mathbf{W}}_t^{(MPC)} = \frac{\sqrt{P_{tot}}\mathbf{W}_t}{\sqrt{N_F \max_j \left[\mathbf{W}_t \mathbf{W}_t^H\right]_{j,j}}} \tag{12}$$

$$\begin{aligned} \hat{\mathbf{W}}_t &= \frac{1}{\sqrt{N_F}} \mathbf{W}_t \left(\text{diag}\left(\text{diag}\left(\mathbf{W}_t^H \mathbf{W}_t\right)\right)\right)^{-\frac{1}{2}} \\ \tilde{\mathbf{W}}_t^{(PAC)} &= \sqrt{\frac{P_{tot}}{N_F}} \left(\text{diag}\left(\text{diag}\left(\hat{\mathbf{W}}_t \hat{\mathbf{W}}_t^H\right)\right)\right)^{-\frac{1}{2}} \hat{\mathbf{W}}_t \end{aligned} \tag{13}$$

In (13), $\hat{\mathbf{W}}_t$ is a support variable that introduces an equal power per-user normalization; the traditional PAC technique is then applied to normalize the row vectors.

III. User Scheduling through Graph Coloring

In our proposed user scheduler, an undirected and unweighted graph $\mathcal{G} = (\mathcal{V}, \mathcal{E})$ is built, where each node in set $\mathcal{V}$ corresponds to a user and each edge in set $\mathcal{E}$ reflects the distance between the corresponding pair of users, *i.e.*, an edge between user i and j exists if their GCD is greater than a predefined threshold. Through the graph representation, the user scheduling task can be mapped into a Minimum Clique Cover (MCC) problem, *i.e.*, a search for the minimal set of cliques that covers the entire graph, as shown in Fig. 3. In a second step, only the $T_{\max}$ largest cliques are considered for scheduling, to maximize the resource usage within the scheduling frame.

By using Haversine formula, the GCD between each pair of users (i, j) can be computed and stored in a distance matrix $\mathbf{\Gamma}$:

$$\begin{aligned} [\mathbf{\Gamma}]_{i,j} &= 2r \arcsin\left(\sqrt{\gamma_{i,j}}\right), \\ \gamma_{i,j} &= \sin^2\left(\frac{\phi_j - \phi_i}{2}\right) + \cos\phi_i \cdot \cos\phi_j \cdot \sin^2\left(\frac{\lambda_j - \lambda_i}{2}\right) \end{aligned} \tag{14}$$

where $\gamma_{i,j}$ is a support variable for clarity purposes and (ϕ_i, λ_i) are the latitude and longitude coordinates of the i-th user, and similarly, (ϕ_j, λ_j) for user j. Then, to obtain the unweighted graph, an adjacency matrix $\mathbf{A}$ is extracted from $\mathbf{\Gamma}$ by using a properly set threshold δ_D:

$$[\mathbf{A}]_{i,j} = \begin{cases} 1 & \text{if } [\mathbf{\Gamma}]_{i,j} \geq \delta_D \\ 0 & \text{otherwise} \end{cases} \tag{15}$$

The MCC problem is NP-hard in general [13], therefore we will focus on a heuristic approach. In [7]–[9] we focused on an iterative maximum clique search and removal approach, by using a branch-and-bound algorithm to find the maximum clique at each step. Since the former approach does not necessarily guarantee the MCC and it is computationally expensive for dense graphs, here we tackle the MCC problem by mapping it into a graph coloring problem on the complementary graph $\mathcal{G}_c$. The objective is to assign the minimum number of colors to graph nodes under the constraint that the same color cannot be assigned to two connected nodes. Indeed, assigning different colors to adjacent vertices on the complementary graph results in a partition of the original graph. We obtain the complementary adjacency matrix $\mathbf{A}_c$ as follows:

$$\mathbf{A}_c = \mathbf{J}_K - \mathbf{A} - \mathbf{I}_K, \tag{16}$$

where $\mathbf{J}_K$ is a $K \times K$ all-ones matrix. $\mathcal{G}_c$ can then be built from the set of users $\mathcal{U}$ (corresponding to the set of vertices $\mathcal{V}$, with $|\mathcal{V}| = K$) and the complementary adjacency matrix $\mathbf{A}_c$ (representing the set of edges $\mathcal{E}_c$). Extensive literature has been produced on graph coloring [14]; in this work, we implement the DSatur algorithm [15] due to its $O((K + |\mathcal{E}_c|) \cdot \log_2 K)$ complexity [14]. This algorithm performs a greedy color search on each vertex, implementing a queuing system to give priority to vertices with higher saturation degree (*i.e.*, with a larger number of colors used for adjacent vertices) and edge degree. The pseudocode of DSatur is outlined in Algorithm 1. In particular, the algorithm uses the following functions:

- FirstElement($\mathcal{Q}$): returns the first element in the sorted set $\mathcal{Q}$;
- GreedyColoring(v): performs a greedy coloring strategy on vertex v, *i.e.*, looks for an already assigned color that is not assigned to any vertex adjacent to v and returns such color if the search is successful, otherwise it returns a new color;
- Saturation(a): returns the saturation of vertex a, *i.e.*, the number of distinct colors assigned to vertices adjacent to a.

It must be noted that, from the user scheduling point of view, the value of δ_D represents the minimum inter-user distance required by the system to simultaneously serve two users through SDM. Clearly, a larger δ_D value will result in a sparser adjacency matrix $\mathbf{A}$ and, hence, a denser complementary graph $\mathcal{G}_c$. Nonetheless, $\mathcal{G}_c$ is typically sparse (*i.e.*, $K \gg |\mathcal{E}_c|$) due to the large satellite coverage areas; hence, the algorithm's complexity can be approximated to $O(K \cdot \log_2 K)$. We refer to this algorithm as Distance-based MCC with DSatur (D-MCC-DSatur). We report in Fig. 4 an example of the geographical distribution of the users scheduled within the same time slot.

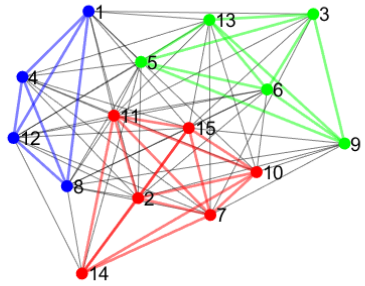

Fig. 3. Graph with $|\mathcal{V}| = 15$ vertices partitioned into 3 cliques.

Algorithm 1 DSatur algorithm pseudocode

Input: Graph $\mathcal{G}_c = (\mathcal{V}, \mathcal{E}_c)$
Output: Cluster sets $\mathcal{C}_t$
Initialize $\mathcal{Q} = \mathcal{V}$
Sort $\mathcal{Q}$ based on decreasing edge degree
while $\mathcal{Q} \neq \varnothing$ **do**
  v = FirstElement($\mathcal{Q}$)
  if v is not colored **then**
    t =GreedyColoring(v)
    $\mathcal{C}_t \leftarrow \mathcal{C}_t \cup v$
    for each node a adjacent to v **do**
      if a is not colored **and** $t \notin$ Saturation(a) **then**
        Saturation(a) $\leftarrow$ Saturation(a) $\cup\, t$
        Insert a as first element in $\mathcal{Q}$
      end if
    end for
    Remove v from $\mathcal{Q}$
  end if
end while

IV. Benchmark: Distance-based MADOC

As a benchmark to evaluate the proposed algorithm, we consider the Distance-based MADOC (D-MADOC) scheduler we presented in [16], which is a location-based variation of the original CSI-based MADOC algorithm [6]. In the distance-based version of the algorithm, $T_{\text{init}} = K/N_F$ groups are initialized, each containing one of the T_{init} users with the shortest slant range. The remaining users are sorted by increasing slant range and each of them is assigned to a group according to the GCD matrix $\mathbf{\Gamma}$. Specifically, the minimum GCD between user i and all of the users belonging to group t, $\Gamma^{(t)}_{\text{min},i} = \min_{j \in \mathcal{C}_t} [\mathbf{\Gamma}]_{i,j}$ is extracted for each group. Then, user i is either assigned to the group with largest $\Gamma^{(t)}_{\text{min},i}$ if such value is higher than a predefined threshold ϵ_D, otherwise it is assigned to an additional empty group. Hence, the distance-based MADOC algorithm provides a partition of the set of users into $T_{\text{MADOC}} \geq T_{\text{init}}$ groups. Nonetheless, as for the proposed algorithm, due to the limited scheduling frame, only the largest $T_{\max}$ clusters are scheduled. From the complexity point of view, the initial sorting requires $O(K \cdot \log_2 K)$ operations. However, the complexity of the algorithm is dominated by

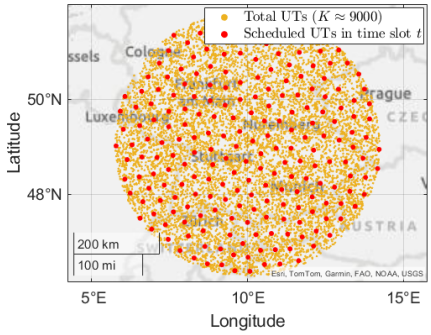

Fig. 4. Distribution of total users and scheduled users in a single time slot in the coverage area.

TABLE II
SIMULATION PARAMETERS.

Parameter	Value
Carrier frequency	20 GHz
System band	Ka (400 MHz)
Beamforming space	Feed
Receiver type	VSAT
Receiver antenna gain	39.7 dBi
Noise figure	1.2 dB
Propagation scenario	Line of Sight (LOS)
System scenario	Urban
Total on-board power density, $P_{t,\text{dens}}$	4 dBW/MHz
Coverage area (spherical cap)	338120 km^2
User density	0.03 user/km^2
No. of time slots $T_{\max}$	20
Number of transmitters N_F	1024 (32×32 UPA)
Monte Carlo iterations	100

the cluster assignment phase: indeed, in the worst case, $k-1$ clusters will have already been generated during the cluster assignment for user k, resulting in $k-1$ comparisons. Hence, the D-MADOC algorithm requires a number of operations $O(\sum_{k=2}^{K} k) = O(\frac{K(K-1)}{2}) = O(K^2)$.

V. SIMULATIONS AND RESULTS

This section presents the outcomes of extensive numerical assessments with parameters specified in Tab. II. The analysis was carried out on the MATLAB environment by means of Monte Carlo simulations. The key considerations are:

- Standalone LEO satellite (600 km from Earth)
- LEO equipped with a UPA of 32×32 feeds
- Coverage area is set to 338120 km^2
- Fixed VSATs
- $T_{\max} = 20$ slots in a scheduling frame to simulate infinite traffic demand.

All the simulation parameters are based on [11], [12].

To maximize the system performance, we perform a heuristic optimization of thresholds for both schedulers (D-MCC-DSatur and D-MADOC) based on the maximization of the average per-cluster sum-rate capacity. Fig. 5 shows that, for each considered power normalization, the sum-rate capacity

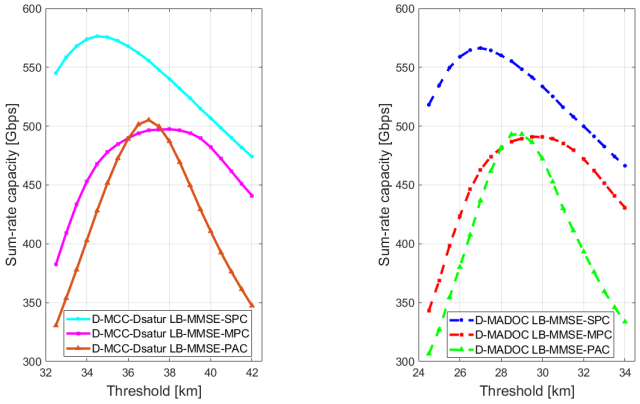

(a) D-MCC-DSatur. (b) D-MADOC.

Fig. 5. Threshold optimization for D-MCC-DSatur and D-MADOC.

TABLE III
SIMULATION RESULTS FOR THRESHOLD OPTIMIZATION

Parameters		D-MADOC	D-MCC-DSatur
Optimized threshold [km]	SPC	27	34.5
	MPC	29.5	38
	PAC	29	37
Mean cluster size	SPC	210.65	216.97
	MPC	185	183.04
	PAC	189.61	191.84
Sum-rate capacity [Gbps]	SPC	566.36	576.45
	MPC	491.09	497.42
	PAC	493.18	502.21

trend is similar between D-MADOC and the proposed D-MCC-DSatur algorithm. Tab. III reports the mean cluster size for each combination of scheduler and power normalization. It is worth mentioning that D-MCC-DSatur forms larger clusters with a greater inter-user distance (the optimal threshold is about 8 km larger for D-MCC-DSatur): clearly, the larger per-cluster sum-rate capacity can be justified by the larger mean cluster size that the graph coloring strategy achieves at least for SPC and PAC; on the other hand, the gain with MPC normalization is due to an increased user orthogonality (larger inter-user distance in each cluster), as D-MCC-DSatur provides on average smaller groups than D-MADOC. We further confirm our results by comparing the average sum-rate capacity that the two schedulers achieve as a function of the mean cluster size. The plot reported in Fig. 6 shows that D-MCC-DSatur outperforms D-MADOC at each considered mean cluster size, with larger clusters providing larger gains.

The Cumulative Distribution Functions (CDFs) of the per-cluster sum-rate capacity achieved with the considered schedulers and power normalizations are reported in Fig. 7. Regardless of the power normalization, the proposed algorithm provides consistent gains over D-MADOC despite the lower complexity. Specifically, D-MCC-DSatur achieves a median sum-rate capacity of 497.42 Gbps with MPC, a 1.29% gain over the state-of-the-art scheduler. The improvement is even larger for the remaining power normalizations, with the pro-

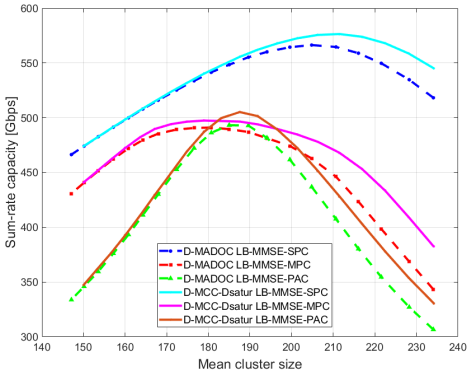

Fig. 6. Mean cluster size vs. per-cluster sum-rate capacity for D-MCC-DSatur and D-MADOC schedulers.

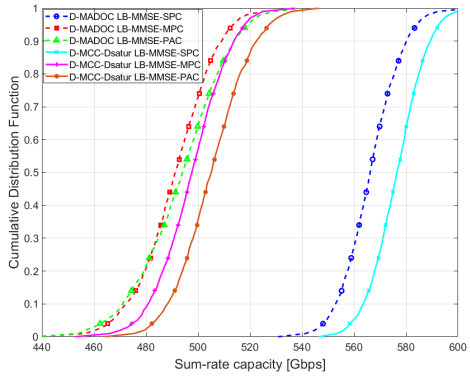

Fig. 7. CDF of the per-cluster sum-rate capacity.

posed algorithm achieving a median sum-rate capacity of 502.21 Gbps (1.83% gain) with PAC and 576.45 Gbps (1.78% gain) with SPC. It is worth noting that the proposed algorithm does not require higher complexity to grant such sum-rate capacity improvements. On the opposite, the computational complexity is reduced with respect to MADOC's, from $O(K^2)$ to $O(K \cdot log_2(K))$. Furthermore, the implementation of the distance-based scheduler and beamformer leads to a reduction in overhead, as both algorithms do not require the transmission of DL pilots to obtain DL CSI, but only the position of the UTs. Future works may focus on assessing the impact of positioning accuracy on distance-based user schedulers, addressing the trade-off between performance and privacy.

VI. Conclusion

In this paper, we presented a novel distance-based user scheduling algorithm based on graph coloring. Both the scheduler and the digital beamformer do not rely on DL CSI, but are instead based on the knowledge of the UT positions, reducing the overall signaling overhead. By coloring the complementary distance-based adjacency matrix using the DSatur algorithm, the MCC problem is solved with lower computational complexity than the state-of-the-art D-MADOC algorithm. The proposed algorithm achieves performance gains in terms of average per-cluster sum-rate capacity over D-MADOC, varying between 1.3% and 1.8% depending on the implemented power normalization technique.

Acknowledgment

This work has been funded by the 6G-NTN project, which received funding from the Smart Networks and Services Joint Undertaking (SNS JU) under the European Union's Horizon Europe research and innovation programme under Grant Agreement No 101096479. The views expressed are those of the authors and do not necessarily represent the project. The Commission is not liable for any use that may be made of any of the information contained therein.

References

[1] 3GPP, "TS 38.108 - NR; Satellite Access Node radio transmission and reception", Jan. 2024.

[2] E. Castaneda, A. Silva, A. Gameiro, and M. Kountouris, "An Overview on Resource Allocation Techniques for Multi-User MIMO Systems", *IEEE Communications Surveys & Tutorials*, vol. 19, no. 1, pp. 239-284, 2017.

[3] P. Angeletti and R. De Gaudenzi, "A Pragmatic Approach to Massive MIMO for Broadband Communication Satellites," in *IEEE Access*, vol. 8, pp. 132212-132236, 2020.

[4] X. Yi and E. K. S. Au, "User Scheduling for Heterogeneous Multiuser MIMO Systems: A Subspace Viewpoint", in *IEEE Transactions on Vehicular Technology*, vol. 60, no. 8, pp. 4004-4013, Oct. 2011

[5] H. Chen and C. Qi, "User Grouping for Sum-Rate Maximization in Multiuser Multibeam Satellite Communications", *ICC 2019 - 2019 IEEE International Conference on Communications (ICC)*, 2019, pp. 1-6, doi: 10.1109/ICC.2019.8761875.

[6] K. -U. Storek and A. Knopp, "Fair User Grouping for Multibeam Satellites with MU-MIMO Precoding," *GLOBECOM 2017 - 2017 IEEE Global Communications Conference*, 2017, pp. 1-7.

[7] D. G. Riviello, B. Ahmad, A. Guidotti and A. Vanelli-Coralli, "Joint Graph-based User Scheduling and Beamforming in LEO-MIMO Satellite Communication Systems," *2022 11th Advanced Satellite Multimedia Systems Conference and the 17th Signal Processing for Space Communications Workshop (ASMS/SPSC)*, 2022, pp. 1-8.

[8] B. Ahmad, D. G. Riviello, A. Guidotti and A. Vanelli-Coralli, "Graph-Based User Scheduling Algorithms for LEO-MIMO Non-Terrestrial Networks," *2023 Joint European Conference on Networks and Communications & 6G Summit (EuCNC/6G Summit)*, Gothenburg, Sweden, 2023, pp. 270-275.

[9] B. Ahmad, D. G. Riviello, A. Guidotti and A. Vanelli-Coralli, "Improved Graph-Based User Scheduling For Sum-Rate Maximization in LEO-NTN Systems," *2023 IEEE International Conference on Acoustics, Speech, and Signal Processing Workshops (ICASSPW)*, Rhodes Island, Greece, 2023, pp. 1-5.

[10] ITU-R Radiocommunication Sector of ITU, "Modelling and simulation of IMT networks and systems for use in sharing and compatibility studies (M.2101-0)", Feb. 2017.

[11] 3GPP, "TR 38.811 - Study on New Radio (NR) to support non-terrestrial networks (Release 15)", Sep. 2020.

[12] 3GPP, "TR 38.821 - Solutions for NR to support non-terrestrial networks (NTN)", May 2021.

[13] V. Verteletskyi, T.-C. Yen, A. F. Izmaylov, "Measurement optimization in the variational quantum eigensolver using a minimum clique cover," in *J. Chem. Phys.*, 152 (12): 124114, 2020.

[14] R. Lewis, "A Guide to Graph Colouring: Algorithms and Applications (second ed.)," 2021, Springer.

[15] D. Brélaz, "New methods to color the vertices of a graph," *Communications of the ACM*, vol. 22, no. 4, pp. 251–256, 1979.

[16] B. Ahmad, D. G. Riviello, B. De Filippo, A. Guidotti and A. Vanelli-Coralli, "Analysis of Graph-based User Scheduling for Ka-band LEO NTN Systems," *28th Ka and Broadband Communications Conference (Ka) and the 40th International Communications Satellite Systems Conference (ICSSC)*, Bradford, United Kingdom, 2023.